Reprinted from Journal of Materials Research, Volume 18, Pages 2697-2707, Copyright 2003, with permission from Materials Research Society.
http://www.mrs.org/publications/jmr/

Effects of surface treatment on the adhesion of copper to a hybrid polymer material

J. Ge[a] and M.P.K. Turunen
Laboratory of Electronics Production Technology, Helsinki University of Technology, Helsinki, Finland

M. Kusevic
VTT Electronics, Oulu, Finland

J.K. Kivilahti
Laboratory of Electronics Production Technology, Helsinki University of Technology, Helsinki, Finland

(Received 25 March 2003; accepted 18 August 2003)

The effects of various surface pretreatments on the adhesion of electroless and sputter-deposited copper metallizations to a hybrid polymer material were investigated. Without pretreatment, the adhesion between copper and the polymer was virtually zero. The adhesion of electroless copper to the polymer was poor regardless of the pretreatment used. However, the wet-chemical pretreatment of the polymer surface markedly increased the adhesion of sputtered copper to the polymer. It preferentially removed the inorganic part of the polymer and formed micropores on the surface. The plasma and reactive ion etching pretreatments, in turn, selectively etched away the organic part of the polymer and noticeably increased the hydrophilicity. Although this resulted in even higher increase in the surface free energy than was achieved with the chemical treatment, the granular surfaces became mechanically brittle. With the help of x-ray photoelectron spectroscopy, scanning electron microscopy, atomic force microscopy, and contact-angle measurements and with the recently developed pull test, the physicochemical changes of the wet-chemically pretreated polymer surfaces were demonstrated to have significant effects on the adhesion.

I. INTRODUCTION

Although many advanced interconnection and packaging technologies as well as high-density microvia boards are already available, the rapidly increasing performance and functionality requirements of wireless devices, in particular, demand the development and implementation of disruptive materials and manufacturing solutions. One such solution is to integrate silicon chips and passive components with very-high-density copper wiring into build-up substrates. This can be realized either by the fully additive or semiadditive techniques utilizing photodefinable polymers and chemical metal-deposition processes.[1–4] On the other hand, to overcome signal integrity problems and other system performance limitations encountered in very-high-frequency applications, an increasing amount of research is being carried out for employing also optical interconnections at the printed circuit board level.[5–7] The technologies enabling the integration of optical and electrical functions in the same polymer substrate implies, among other things, the usage of most advanced photoimagable materials such as inorganic–organic hybrid polymer materials being synthesized with the sol-gel technology.[8,9] These materials combine many useful characteristics of polymers and inorganic solids together with excellent optical properties, and therefore they appear exceptionally attractive for the integration of optical waveguides into high-density multilayer printed wiring boards; the technology that is gaining increasing importance in manufacturing advanced electronics.[1,2]

It is to be noted, however, that the technological advantages provided by the highly integrated electronic and optoelectronic build-up modules depend not only on the advanced materials and fabrication processes but also—and often primarily—on good adhesion between the thin sequential layers of dissimilar materials.[10–12] The last requirement is particularly difficult to fulfill in the case of copper and the hybrid polymer materials having highly cross-linked structure.

[a]Address all correspondence to this author.
e-mail: ge.jun@hut.fi

 © 2003 Materials Research Society

To improve the adhesion, the most frequently used method is to roughen the surface of polymer by wet-chemical treatments.[13,14] As a result, the mechanical anchoring of electrolessly deposited copper can occur inside the fine cavities of the roughened polymer surface. However, there are an increasing number of applications in which the roughened polymer surfaces have a deleterious effect on the electrical performance, especially in high-frequency applications.[15,16]

An alternative metallization method is the dry process, which includes plasma or reactive ion etching (RIE) pretreatment followed by the sputter-deposition of copper onto the activated surface. The pretreatment is performed to modify the surface chemistry and morphology of the polymer. To achieve the adhesion improvement, only the outermost surface layer is to be affected while the bulk polymer and its properties are left unaltered. This technique has the advantage of being able to achieve sufficient adhesion to smooth surfaces.[17,18]

To the best of our knowledge, no study has been carried out on the adhesion of deposited copper to inorganic–organic hybrid materials. Therefore, in the current work the effects of the wet-chemical, plasma, the combination of both, and the RIE pretreatments on the adhesion of deposited copper to an inorganic–organic hybrid polymer material were investigated. The physicochemical changes on the polymer surfaces were characterized with x-ray photoelectron spectroscopy (XPS), atomic force microscopy (AFM), and contact-angle measurements, and the failure modes were examined with optical microscopy and scanning electron microscopy (SEM).

II. EXPERIMENTAL

A. Materials and methods

E-glass reinforced epoxy (FR4 from NELCO, United Kingdom) was used as the base substrate. The photodefinable sol-gel material (produced by VTT Electronics, Oulu, Finland) was spin-coated onto the base substrate to a thickness of approximately 10 μm. After spin coating, the board was soft-baked at 70 °C for 5 min, ultraviolet (UV) exposed (13.3 mW/cm^2), and finally cured at 140 °C for 10 h. Inorganic–organic copolymerization principle is based on the sol-gel techniques. The organic moieties react with the inorganic precursors and chemically bond to the inorganic sol-gel network. During sol-gel processing, the inorganic network is formed first and upon ultraviolet exposure, the acrylic double bonds start to cross-link (Fig. 1). As a result, the polymer acts as a photodefinable negative resist material.

The sample preparation method is schematically shown in Fig. 2. Three different surface modification methods were evaluated for the pretreatment of the polymer. The wet-chemical treatment consists of three water-based steps: swelling (3 min at 65 °C), etching (5–30 min at 70 °C), and reduction (2 min at 25 °C).[19] In the second pretreatment, a barrel-type plasma reactor was used. Samples were placed in the substrate holder surrounded by a tunnel-perforated metal shield between samples and electrodes. The conditions for the plasma treatment were as follows: the gas source was oxygen, the frequency was 13.56 MHz, the treatment period varied from 5 to 25 min, the rf power was 80 W, and the gas pressure was 26 Pa. In addition, the result of the combination treatment of sequential plasma and wet-chemical etching was studied. In this procedure, the exposure time of the sample with plasma was fixed at 5 min, and the etching time in the chemical treatment was changed from 5 to 20 min with 5-min steps. The third surface modification method was reactive ion etching, using a parallel plate reactor. Plasma in the RIE system was produced in the region between two electrodes, and the sample was placed directly below the plasma, on a plate shielding the lower electrode, which was powered by a 13.56-MHz radio-frequency (rf) generator. The surface modification was performed with an O_2 flow rate of 15 sccm. The rf power was fixed at 80 W, and the operating pressure was held at 2.7 Pa. The treatment time ranged from 5 to 25 min.

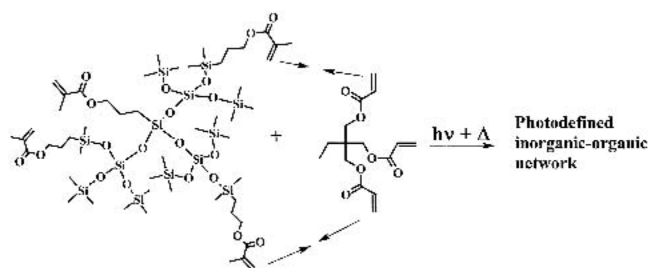

FIG. 1. A schematic representation of the cross-linking of the inorganic–organic hybrid material.

The treated surface was then metallized electrolessly or by the sputter-deposition of copper to a thickness of 1 μm. The electroless plating is a wet chemical deposition process and the copper deposition is the result of redox reactions. The treated samples were immersed (5 min at 45 °C) in the catalyst solution (Circuposit TM 3344, Shipley, United Kingdom) containing colloidal palladium–tin particles. After the activation step, the samples were rinsed with the distilled water to remove the excess Pd/Sn particles and immersed (15 min at 36 °C) in the electroless plating solution (Cuprothick 84, Alfachimici, Italy). The solution consists of an aqueous copper sulfate solution and formaldehyde. Copper metal deposits by copper cation reduction on the polymer surface with the plating rate of 4–5 μm/h. In the case of sputter-deposition, the samples were processed under vacuum in the following conditions: base pressure = 1.5×10^{-4} Pa, work pressure = 0.43 Pa, dc power = 2000 W, and

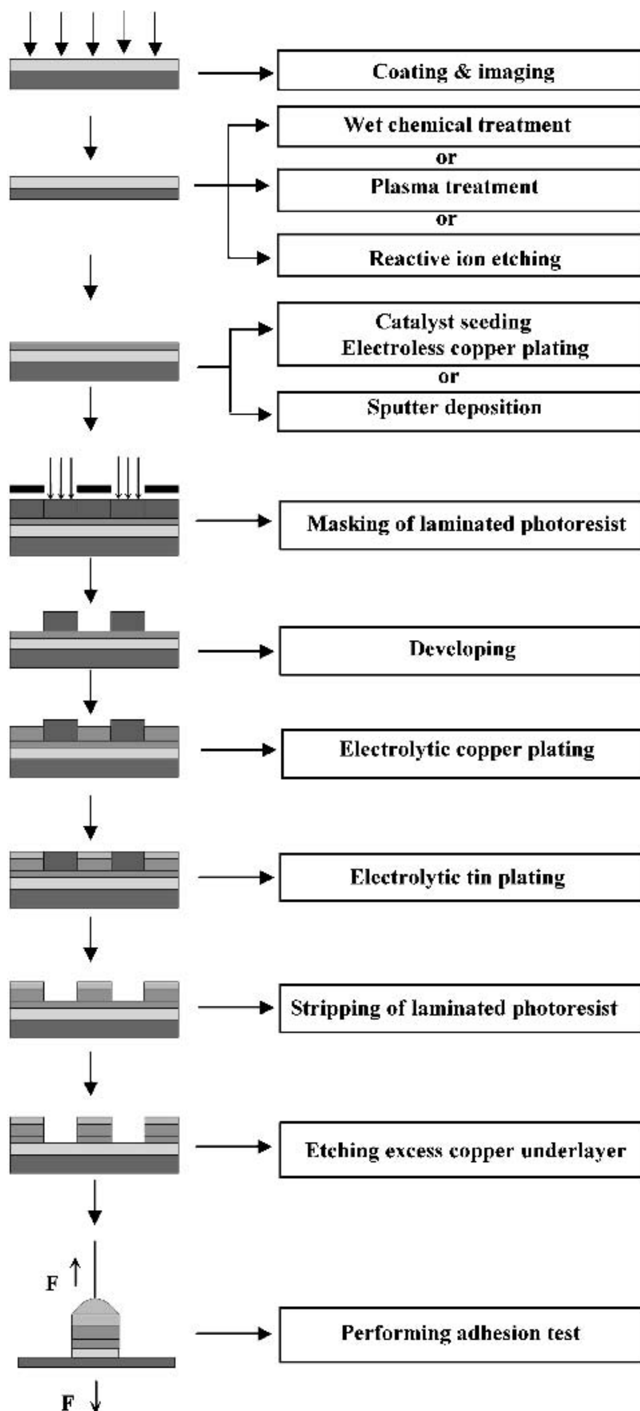

FIG. 2. Schematic representation of the sample preparation method for the pull test.

argon gas rate = 60 sccm. The results shown in this study are from the sputter-deposited copper unless otherwise stated.

After metallization, a dry film type of photoresist was laminated onto it and exposed through a photo mask. The trench structure of the resist was formed by developing. Copper was then electrolytically plated onto the electroless or sputter-deposited copper that was revealed at the bottom of the resist trenches so as to achieve a thicker copper layer. As an etching resist, a tin layer was electrolytically plated onto the copper surface, and the dry film photoresist was then stripped off. Finally, the excess copper was removed with copper etching solution (Ultraincide 35/35 from Alfachimici, Italy) to form test pads with a diameter of 2 mm. The adhesion test pads with sufficient surrounding substrate were then cut out from the fabrication panel. Copper wire was finally microsoldered to the test pads with a eutectic SnPb solder for attachment to the pull test equipment (Fig. 2).

B. Characterization

The adhesion was measured by the recently developed pull test[19] and qualitatively by the more simple tape test according to the IPC-MF-150 standard. The MTS 858 tensile test machine was used to measure the pull strength (i.e., the adhesion of Cu to the hybrid material). The specimen was fixed to the test set-up, and a copper wire was then clamped in the grip and pulled at a constant ramp rate of 0.001 mm/s. The force required to break the weakest interface was recorded. The test pad area was calculated by assuming that the pad was circular. The pull strength was evaluated as the average tensile strength of the 12 specimens prepared under the same conditions. The details of the test configuration has been reported elsewhere.[11,19]

The topographies of the treated surfaces (tilted at 45°), as well as the fracture surfaces of the metallized polymer after the pull test, were examined using a field-emission scanning electron microscope equipped with an energy dispersive spectrometer (JSM-6330F, JEOL, Tokyo, Japan) operated at 1 kV or 15 kV.

The surface topography of the untreated and treated material was characterized on a Nanoscope IIIa atomic force microscope (Digital Instruments D3100, Santa Barbara, CA). In each case, an area of 3×3 μm was scanned using silicon tips in the tapping mode. The surface roughness of the samples was evaluated in terms of the arithmetic mean of the roughness (Ra) and the root mean square (rms) roughness.

The contact angles of water, diiodomethane (DIM), and formamide (FA) on the hybrid material were measured by the sessile drop method with a video contact angle system (model VCA 2500XE, Advanced Surface Technology Inc., Billerica, MA). For each sample, the contact angle value is the average of eight measurements recorded from different locations on the sample surface with a standard deviation of 1° to 3°. From the measured contact angles, the surface free energy (γ_s) was calculated using the geometric mean model.[20,21] The volume of the liquid drop was 0.1 μl. The dispersive (d) and polar (p) components of the surface tension of the different liquids (γ_L) adopted herein for geometric mean model are $\gamma_L = 72.8$ mJ/m^2, $\gamma_L^d = 21.8$ mJ/m^2, and

$\gamma_L{}^p$ = 51.0 mJ/m^2 for distilled water and γ_L = 50.8 mJ/m^2, $\gamma_L{}^d$ = 49.5 mJ/m^2, and $\gamma_L{}^p$ = 1.3 mJ/m^2 for diiodomethane.[20,22]

The x-ray photoelectron spectra of both the untreated and treated hybrid materials were recorded using an AXIS 165 XPS (Kratos Analytical, New York). The monochromatic Al K_α x-ray source was operated at an anode voltage of 12.5 kV and a current of 8 mA. Survey spectra were acquired from 0 to 1100 eV, with a pass energy of 80 eV and a step size of 1 eV being used. The core level spectra were obtained with a pass energy of 20 eV and a step size of 0.1 eV being used. A photoelectron take-off angle of 90° was used for all the analyses. All XPS peaks were referenced to a C1s signal at a binding energy of 285 eV, representing the C–C and C–H bonds in hydrocarbons.

III. RESULTS AND DISCUSSION

The samples that were pull-tested were metallized chemically using aqueous solution or else they were sputter-deposited in the vacuum system. The results of the tests are given in Table I. The plasma (or reactive ion etching) pretreatment alone is not sufficient to obtain acceptable adhesion from the reliability point of view. The highest pull strength (6.6 MPa) is achieved for the sputter-deposited Cu/polymer system pretreated by the combination of plasma and chemical methods. Comparable pull strength values are also obtained with the wet-chemical pretreatment. It should be noted that the electrolessly deposited copper exhibits very poor adhesion to the polymer regardless of the pretreatments. Thus, the adhesion improvement achieved with plasma and chemical pretreatment and the combination of both, followed by the sputter deposition of copper metallization, is emphasized in this study.

A. AFM and SEM

AFM and SEM micrographs of the untreated and treated polymer surfaces are shown in Figs. 3 and 4, respectively. The untreated surface shows a very smooth topography and its rms roughness is 0.8 nm. The pretreatments result in the increase of the rms value of the polymer surfaces (Fig. 5). A uniform granular surface topography is observed after the plasma treatment [Fig. 3(c)]. The chemical treatment, on the other hand, results in a quite different surface morphology. The bright regions in the three-dimensional images of the polymer represent pores that are formed within the heterogeneous material [Fig. 3(b)]. The localized degradation of the hybrid material by the chemical treatment is further increased by preceding plasma treatment, as can be observed by comparing Figs. 3(b) and 3(d). The surfaces treated by the combination of plasma and wet-chemical treatments show a topographically similar appearance to those treated only wet-chemically, but with higher level of the roughness and larger number of micropores. However, the number of pores produced in the surfaces is not sufficient, and the modified surfaces do not serve as a good substrate for chemical deposition of copper.

During the plasma exposure, hydrocarbons on the surface react with the oxygen plasma and form volatile degradation compounds such as CO and CO_2.[23–25] It is expected that when the etching of hydrocarbons takes place, the exposed phase [i.e., the grains seen in Fig. 3(c)] is silicon-based. The sacrificial region between the grains is suggested to be composed of the hydrocarbon-based material that is more easily etched than the grains themselves. In principle, the chemical treatment is an isotropic etching process, but the heterogeneities in the hybrid material enable the formation of a rough surface as the phases are etched at different rates. The reaction is initiated at local oxidizing centers and silicon-containing species are dissolved by the selective etching. As seen in Fig. 4(b), some oval-shaped pits are formed on the surface with 10-min etching time and the surface roughness increases slightly, as compared to the untreated surface [Fig. 4(a)]. However, mechanical interlocking sites are not produced noticeably with the continued etching time. Instead, irregular cracks occur, which lead to the damage of the polymer surface [Fig. 4(c)]. It should be noted that there is no direct correlation between the surface roughness and the measured pull-strength values. Hence, further information about the chemical state of polymer surfaces and wettability must be obtained.

TABLE I. The adhesion of sputter-deposited copper to the hybrid polymer.

Treatments	Tape test	Pull test	Failure modes
Untreated	x	x	Adhesive
Plasma (O_2)	√	x	Adhesive
RIE (O_2)	√	x	Adhesive
Chemical	√	5.6 MPa	Mixed[a]
Plasma + chemical	√	6.6 MPa	Mixed[a]

Fail, x; pass, √; RIE, reactive ion etching.
[a]Adhesive/cohesive.

B. XPS analyses

The XPS widescan spectra of the untreated and treated polymer surfaces are compared in Fig. 6. The induced compositional modification, as obtained by XPS analysis, is based on the experimental peak areas for Si2p, O1s, and C1s which are shown in Fig. 7. The result shows that the plasma treatment induces a pronounced depletion of carbon, from 42% to 11%, and simultaneous

enrichment of Si and O while the chemical treatment and the combination of the two treatments result in a marked but reverse effect, producing a strong decrease of Si from 16% to 5%.

The C1s and O1s can be deconvoluted into several peaks, which characterize the different possible bonding states as shown in Fig. 8. For the C1s core level spectra, the peaks centered at 285, 286.6, 287.7, and 289.4 eV are assigned to C–C, C–O, C = O/C–O–C and O–C = O groups, respectively.[26] The O1s spectrum of the untreated sample is fitted with two main peaks corresponding to Si–O and C–O bonds (BE = 532.4 eV, 84%) and O = C–O bond (BE = 534 eV, 16%), respectively (Table II). The oxygen concentration includes a contribution from O atoms in carbon-containing groups and the Si–O–Si network as well as from those in the Si–OH bonds. A certain amount of SiOH moieties are due to the absorption of water molecules into the surface and subsequent hydrolysis or the incomplete reaction.

After the plasma treatment, the intensity of the peak at 532.4 eV is observed to increase (Fig. 8). The silicon-containing moieties are expected to be the main contribution to the peak, and oxygen is mainly present in the form of Si–O groups. This is because a loss of approximately 30% of carbon is detected while silicon and oxygen increase simultaneously (Fig. 7). Surface hydrocarbons react with the oxygen plasma and are expected to form volatile compounds such as CO and CO_2. The C–O group of the organic portion undergo oxidation to C = O/O–C–O and COOH/COOR. The XPS results strongly indicate that there is a marked compositional modification taking place. The carbon-containing groups

TABLE II. The chemical composition of the untreated and treated polymer surface as detected by XPS.

Functional groups (%)	Binding energy (eV)	Untreated	Chemical	Plasma	Plasma + chemical
C–C	285	53.8	66.5	48.7	67.4
C–O	286.6	24.2	15	19.2	14
C = O/C–O–C	287.7	5.2	···	10.4	···
O = C–O	289.4	16.8	18.5	21.7	18.7
Si–O C–O	532.4	84.2	64.6	92.8	64.6
O = C–O	534.0	15.8	35.4	7.2	35.4

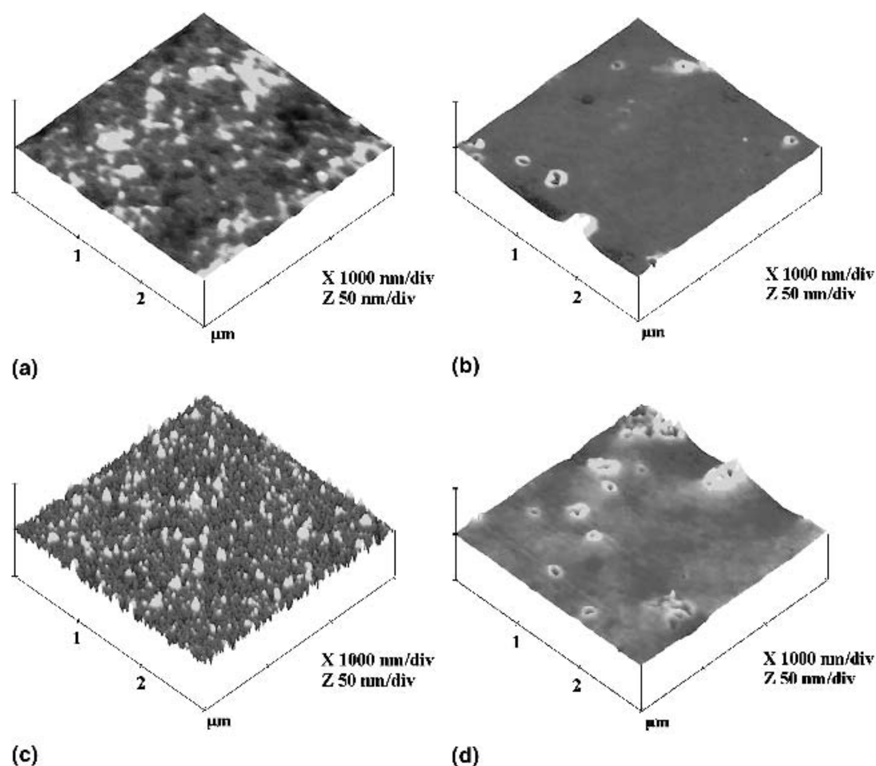

FIG. 3. AFM images of the polymer surfaces (a) untreated, (b) wet-chemically treated, etching time 10 min, (c) plasma treated (5 min), and (d) combination treatment (plasma etching 5 min + wet-chemical etching 5 min).

decrease significantly and the polymer contains relatively large amounts of silicon-containing groups. As a result, the surfaces are expected to be more inorganic after the treatment.

The carbon spectra of the wet-chemically treated surface show a notable increase in the concentrations of the C–C/H and O–C = O peak components. The relative numbers of C–O bonds decrease and C = O almost disappears. The decrease in C–O and C = O is expected to result from the conversion of C–O–C bonds on the polymer to other species (i.e., ester and carboxylic acid) or volatile compounds (CO and CO_2). On the other hand, the chemical treatment leads to an increase in the silanol concentration through the hydrolysis of the surface siloxane bonds to form SiOH groups. The silica species including the Si–O–Si bridge, for example $(OH)_3$Si–O–Si$(OH)_3$, dissolve in the etching solution. The selective etching results in a less dense Si–O–Si network. This probably explains the decrease in the total amount of oxygen and silicon. Similar chemical changes are seen on the surfaces subjected to the combined treatments of plasma and wet chemical etching.

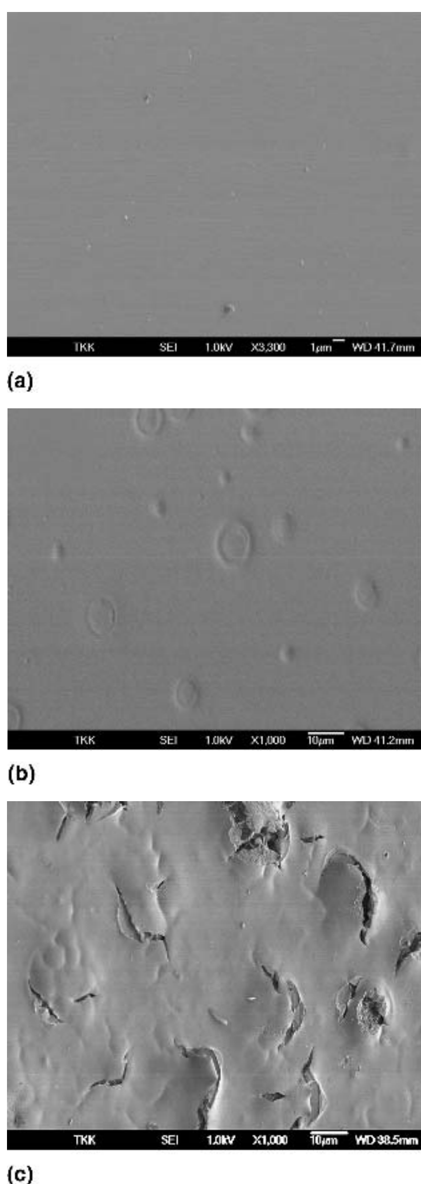

FIG. 4. The surface topography of the polymer as examined with SEM: (a) untreated, wet-chemically etched for (b) 10 min and (c) 25 min.

C. Wettability

To evaluate the changes in the wettability of the modified polymer surfaces, further characterization of the surfaces is made by water and diiodomethane contact-angle measurements and related surface free energy calculations. Although there is no simple relationship between wettability and adhesion, the contact-angle measurements carried out with polar (water) and apolar (DIM)

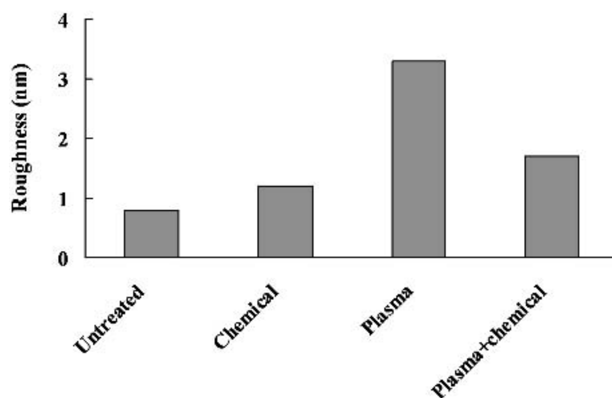

FIG. 5. The roughness (RMS) of the untreated, wet-chemically treated (etching time 10 min), plasma treated (5 min) and plasma + chemically treated polymer surfaces.

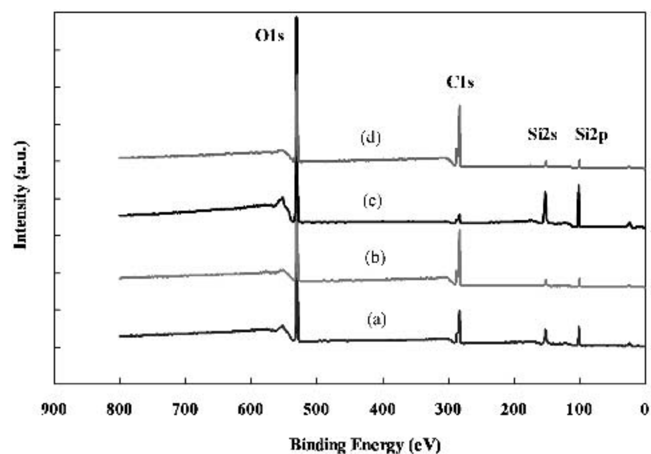

FIG. 6. The XPS wide scan spectra for the polymer (a) untreated, (b) chemically treated (etching time 10 min), (c) plasma treated (5 min), and (d) combination treatment (plasma etching 5 min + wet-chemical etching 5 min).

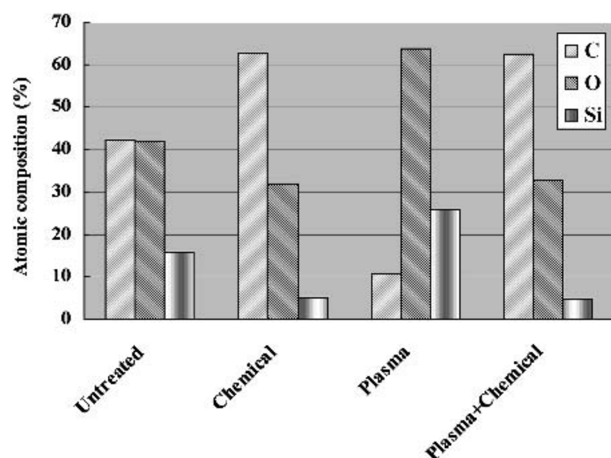

FIG. 7. The composition (at.%) of the polymer as determined by XPS analyses.

probing liquids enable the interpretation of hydrophilicity/hydrophobicity of the material. Improved wettability is generally a result of increased hydrophilicity and the simultaneous increase in surface free energy in the case of polymers. The study of contact angles serves as an additional method to XPS to improve our understanding of the various chemical changes taking place on the surface as a consequence of the modification treatments. The wettability of a polymer depends primarily on the state of the surface; for example, chemistry, polarity, roughness, and chemical heterogeneity.[27–31] The contact angles of water, DIM, and FA on the treated polymer surfaces as a function of the treatment time are shown in Table III. The water contact angles on the wet-chemically and plasma treated polymer surface decrease significantly, from 62° to 44° and to below 10°, respectively, after 5 min of treatment whereas the DIM contact angles remain almost constant.

The plasma treatment results in compositional modification, and the formation of predominant $[SiO_4]_n$ clusters is expected. The symmetry of the siloxane backbone of the inorganic network is disrupted as a result of the treatment, which probably generates dipole moments capable of forming hydrogen bonds with water. Thus, the treated surface appears highly hydrophilic as the water contact angles approach zero. The wet-chemical pretreatment also improves the wettability of the polymer. The geometric-mean model is used in the calculation of surface free energy.[20,32] The surface free energy of the polymer and especially its polar component (γ_S^P) are shown in Table III and Fig. 9. Analysis of the observed changes in the total surface free energy in terms of the polar and dispersive component contributions showed that the strong enhancement of the hydrophilic character of the treated surfaces is mainly due to the increased polar component of surface free energy as compared with the untreated surface. This can be related to the formation of

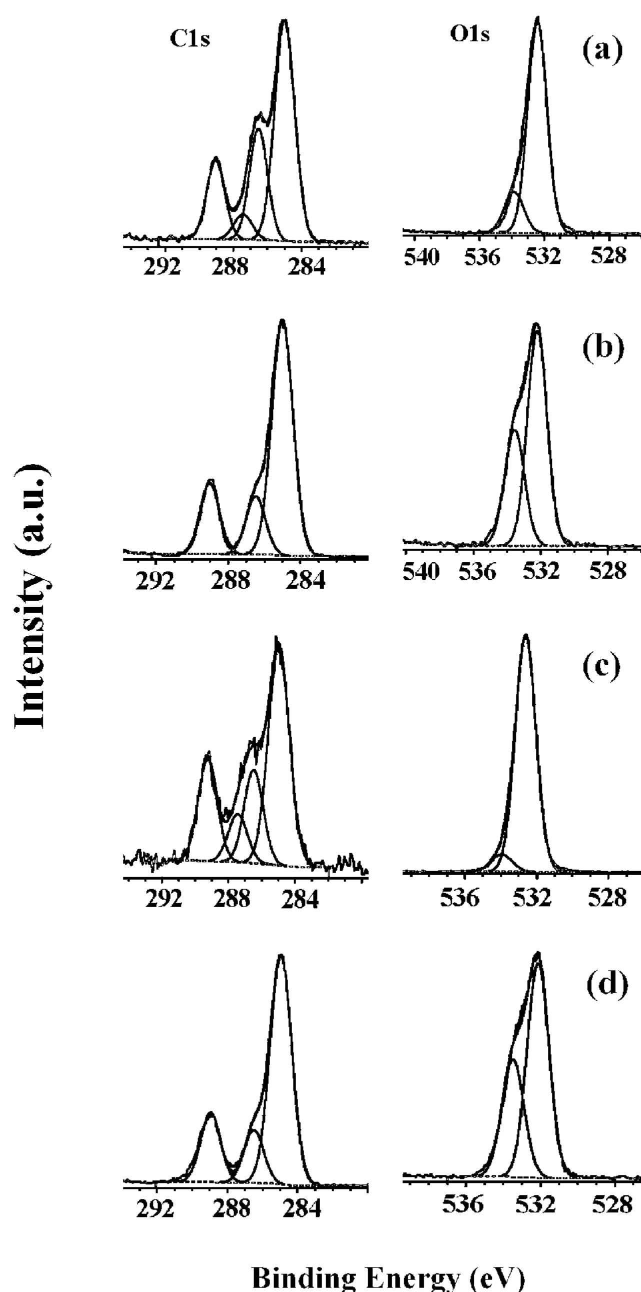

FIG. 8. XPS (C1s, O1s, Si2p) spectra for the polymer surfaces: (a) untreated, (b) chemically treated (etching time 10 min), (c) plasma treated (5 min), and (d) combination treatment (plasma etching 5 min + wet-chemical etching 5 min).

hydrophilic groups on the surface, as detected by XPS. However, the competition between degradation and functionalization reactions limits further increase in the O/C ratio and the surface free energy. It should be noted that the effect of the chemical treatment on the surface polarity is not as strong as that of the plasma treatment. This is because the formation of the $[SiO_4]_n$ clusters sharply increases the hydrophilicity contributing to the increase of the surface free energy.

D. Adhesion

Previously, we have observed that the formation of a sufficient amount of microcavities in the polymer surface is the necessary condition for good adhesion between polymers and electrolessly deposited copper.[11,19] It is to be noted that no significant roughness is produced regardless of the pretreatment. Thus, very poor adhesion is obtained if the electroless copper deposition is used. However, if sufficient chemical activation takes place on the surface, the sputter-deposition, being a high-energy deposition method, leads to good adhesion even on the relatively smooth polymer surface.[10] This, in turn, is essential for achieving the good electrical performance required in high-frequency applications.

The plasma and RIE pretreatments do not improve the adhesion significantly (Table I), whereas wet-chemical pretreatment results in improved adhesion. The pull strength values for the sputter-deposited copper as a function of etching time after both wet-chemical and combined treatments are plotted in Fig. 10. The chemical treatment increases the adhesion and after 10-min treatment the maximum value of 5.6 MPa is obtained with the transition in the failure mode from adhesive to adhesive/cohesive. A decrease of the adhesion follows if the wet-chemical treatment is continued for a long period of time. This is suggested to be the consequence of deteriorated mechanical properties of the polymer and/or the formation of a weak boundary layer (WBL) due to the numerous cracks. In the case of the combined treatment, greater adhesion strength values (over 6.6 MPa) are obtained after an etching time shorter than those used in the chemical treatment alone (Fig. 10).

The differences in the adhesion test results between the plasma and chemically treated surfaces can be rationalized as follows. The plasma pretreatments etch the organic part of the hybrid polymer material and give rise to the progressive enrichment of silicon on the polymer surfaces. The chemical treatment, in contrast, leads to the removal of the silicon-containing groups and the

TABLE III. The contact angles of water and diiodomethane on the treated surface as a function of the treatment time.

Treatments	Time (min)	Contact angle (°)					
		H_2O	DIM	FA	γ^d	γ^p	γ_s
Untreated	⋯	61.6	35.1	22.2	35.7	13.1	48.8
Wet chemical	5	43.6	34.8	<10	33.2	25.2	58.4
	10	47.3	32.8	<10	34.6	22.2	56.8
	20	43.3	36.8	<10	32.2	26	58.2
	30	45.5	35.4	<10	33.2	24.1	57.3
Plasma	5	<10	28.8	<10	32.8	41.6	74.4
	10	<10	32.9	<10	31.1	42.8	73.9
	15	<10	36.3	<10	29.6	44	73.6
	20	<10	30.9	<10	32	42.2	92.3
Plasma + chemical	Plasma (5) + chemical (5)	46.8	33.9	<10	34	22.8	56.8
RIE	5	<10	7.2	<10	29.3	43.9	73.2

DIM, diiodomethane; FA, formamide; RIE, reactive ion etching.

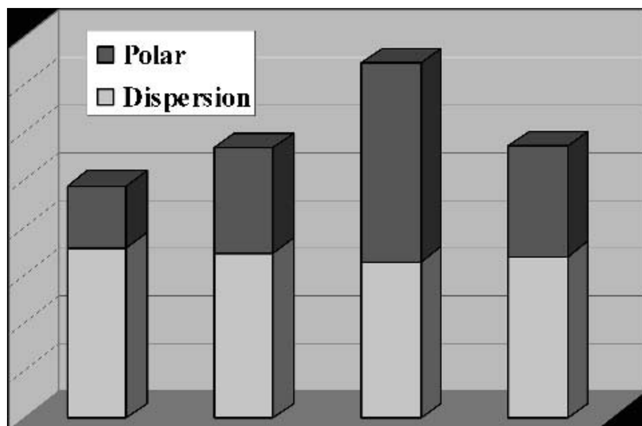

FIG. 9. The components of surface free energy (γ_S) for the untreated and treated polymer. The $\gamma_S{}^d$ and $\gamma_S{}^p$ are dispersion and polar force components of the γ_S, respectively.

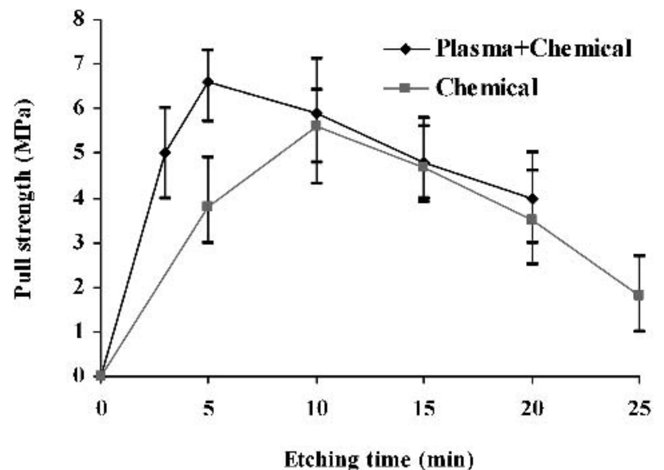

FIG. 10. The pull strength between sputter-deposited copper and the polymer as a function of etching time in the chemical and combination treatments.

formation of oxygen-containing moieties on the polymer surface. It is generally known that charge-transfer complexes are formed between metal films and carbon–oxygen functional groups on polymers and that the presence of these complexes contributes to the adhesion.[33–38] It is expected that the good adhesion achieved in the case of chemical treatment is mainly attributed to the complex formation. The formation of micropores in the surfaces increases the interfacial contact area, and this also contributes to the adhesion. On the other hand, as a result of the plasma treatment, no such complex formation is expected in the copper/polymer systems. This is because the surface chemistry of the polymer is strongly modified, resulting in the formation of $[SiO_4]_n$ clusters. In addition, because of the granular topography of the hybrid material, the surface layer is mechanically brittle. Therefore, no adhesion improvement is obtained after the plasma treatment.

The fracture surfaces of the adhesion test specimens are examined with SEM to identify the failure modes and to provide qualitative assessment of the adhesion of Cu to the polymer. In most cases, the failure occurs as a complete adhesive fracture along the interface between Cu and the polymer [Table I and Fig. 11(a)]. However, when high pull strength values in the copper/polymer system are achieved, the locus of failure is shifted within

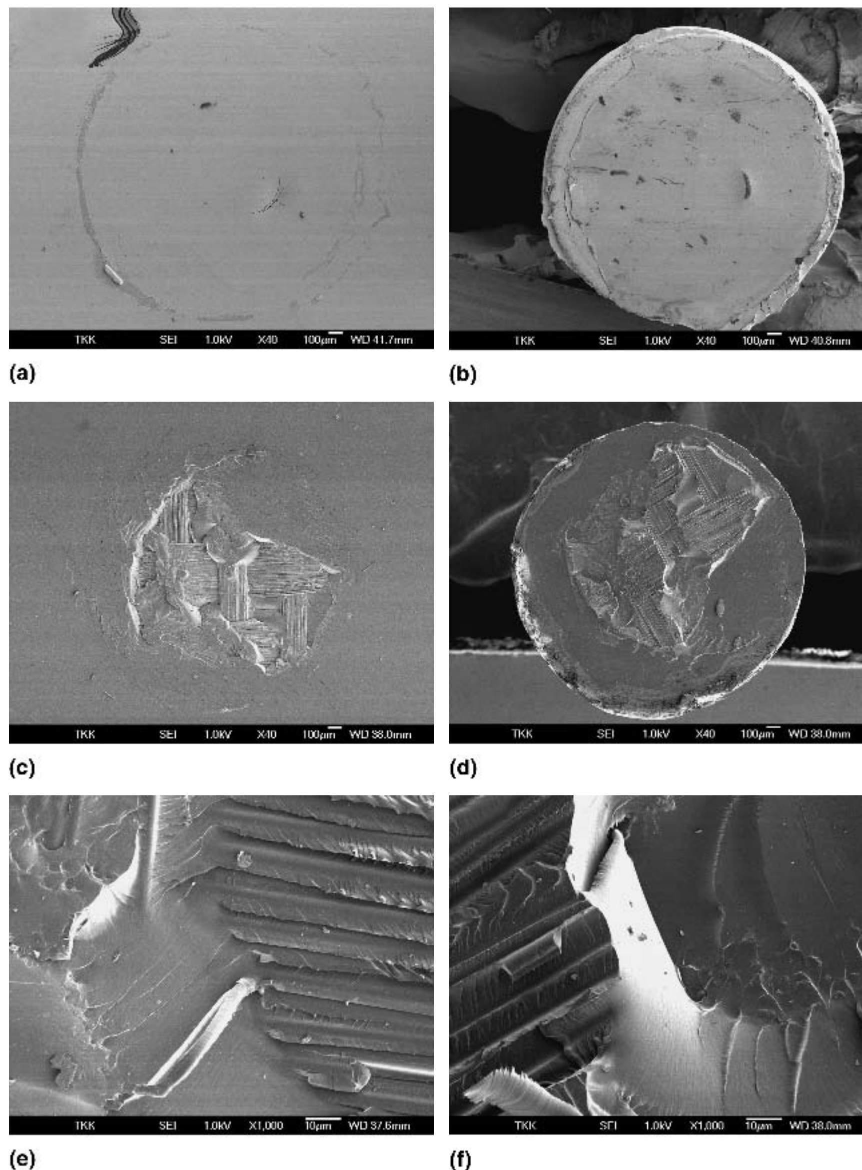

FIG. 11. SEM micrographs of typical fracture surfaces after the pull test. No treatment (a) polymer side, (b) back side of the test pad. Chemical treatment (etching time 10 min) (c) polymer side, (d) back side of the test pad, (e) and (f) higher magnifications of (c) and (d), respectively.

the polymer, further from the interface. In fact, the failure occurs partially inside the FR4 substrate as well; the glass fibers of FR4 can be observed on the polymer side after the pull test [Fig. 11(c)]. Evidently, the adhesion strength is much stronger at the Cu/polymer interface than at the failed site, and the failure is adhesive/cohesive mixed mode. In some cases, fracture occurs at the WBL/bulk interface. This is because the excessive treatment of the polymer results in the formation of weak boundary layer that is easily broken during the adhesion test.

IV. CONCLUSIONS

The effects of chemical and physical pretreatments on the adhesion of electroless and sputtered copper to an inorganic–organic hybrid polymer were investigated. The pretreatments markedly altered the chemical and topographic state of the polymer surface and resulted in distinctly different adhesion results. The wet-chemical treatment increased the content of the organic component on the surface. The selective etching, with the removal of silicon-containing groups from the surface, resulted in the formation of micropores. A similar chemical state of the polymer surface but with more micropores was achieved with the combined plasma and sequential wet-chemical pretreatment. In contrast to this, the plasma and RIE treatments noticeably modified the surface chemistry of the polymer, with the enrichment of silicon. The $[SiO_4]_n$ clusters formed during the pretreatment significantly increased the hydrophilicity. Simultaneously, granular surface topography resulted from the preferential removal of the organic part of the polymer. The modified surfaces appeared mechanically brittle. Thus, the adhesion of sputter-deposited copper to the plasma and RIE treated surfaces was not improved appreciably. However, the wet-chemical pretreatment significantly enhanced the adhesion owing to the advantageous chemical alteration of the surface and the formation of micropores in the polymer surface. When pull strength values in the copper/polymer systems were high, the fracture mode was predominately adhesive/cohesive. The experimental results provided evidence that good wettability is a necessary but not sufficient condition for good adhesion.

ACKNOWLEDGMENTS

The authors would like to acknowledge their gratitude to Ms. Laura Orre from Ashland Finland Oy for providing the equipment for the contact-angle measurements, Leena-Sisko Johansson, Ph.D., for performing the XPS analyses, Kari Lounatmaa, Ph.D., for his contribution to the SEM examinations, and Mr. Kimmo Henttinen from VTT Microelectronics for the AFM measurements. We are also grateful to Dr. Tomi Laurila for his useful comments. The work was financially supported by Academy of Finland.

REFERENCES

1. J.K. Kivilahti, J. Liu, J.E. Morris, T. Suga, and C.P. Wong, in *Proceedings of the 52nd IEEE Electronic Component and Technology Conference,* edited by M. Mcshane and S. Bezuk (IEEE, Piscataway, NJ, 2002), p. 955.
2. R. Tuominen and J.K. Kivilahti, in *Proceeding of the International Conference on the 4th Adhesive Joining & Coating Technology in Electronics Manufacturing,* edited by M. Hyytiainen (Institute of Electrical and Electronic Engineers, NY, 2000), p. 269.
3. S.N. Towle, H. Braunisch, C. Hu, R.D Emery, and J.V. Gilroy, in *ASME International Mechanical Engineering Congress & Exposition*, edited by E.P. Scott and J.C. Bischof (American Society of Mechanical Engineers, New York, 2001), p. 211.
4. T.F. Waris, R. Tuominen, and J.K. Kivilahti, in *Proceedings of the 1st International IEEE Conference on Polymers and Adhesives in Microelectronics and Photonics,* edited by N. Kruse, C. Nieland, and R. Wenzel (IEEE, Piscataway, NJ, 2001), p. 218.
5. E. Griese, IEEE Trans. Adv. Packag. **24,** 375 (2001).
6. Y.S. Liu, R.J. Wojnarowski, W.A. Hennessy, J. Rowlette, J. Stack, M. Kadar-Kallen, E. Green, Y. Liu, J.P. Bristow, A. Peczalski, L. Eldada, J. Yardley, R.M. Osgood, R. Scarmozzino, S.H. Lee, and S. Patra, in *Proceedings of 47th IEEE Electronic Component and Technology Conference,* edited by E.J. Vardaman (IEEE, Piscataway, NJ, 1997), p. 391.
7. K. Schmieder and K-J. Wolter, in *Proceedings of the 50th IEEE Electronic Component and Technology Conference*, edited by T.G. Reynolds III and M. Mcshane (IEEE, Piscataway, NJ, 2000), p. 749.
8. C.J. Brinker and G.W. Scherer, *Sol-Gel Science, the Physics and Chemistry of Sol-Gel Processing* (Academic Press, New York, 1990).
9. D.C. Bradley, R.C. Mehrotra, and D.P. Gaul, *Metal Alkoxides* (Academic Press, New York, 1978).
10. J. Ge and J.K. Kivilahti, J. Appl. Phys. **92,** 3007 (2002).
11. J. Ge, M.P.K. Turunen, and J.K. Kivilahti, J. Polym. Sci. Part B: Polym. Phys. **41,** 623 (2003).
12. J. Ge, M.P.K. Turunen, and J.K. Kivilahti, Thin Solid Films **440,** 198 (2003).
13. C.F. Coombs, *Coombs' Printed Circuits Handbook* (McGraw-Hill, New York, 2001).
14. C.A. Harper, *High Performance Printed Circuit Boards* (McGraw-Hill, New York, 2000).
15. R. Heinz, E. Klusmann, H. Meyer, and R. Schulz, Surf. Coat. Tech. **116–119,** 886 (1999).
16. J.H.C. Van Heuven, IEEE Trans. Microw. Theory Tech. **22,** 841 (1974).
17. K. Harth and H. Hibst, Surf. Coat. Technol. **59,** 350 (1993).
18. F.D. Egitto and L.J. Matienzo, IBM J. Res. Develop. **38,** 423 (1994).
19. J. Ge, R. Tuominen, and J.K. Kivilahti, J. Adhes. Sci. Tech. **15,** 1133 (2001).
20. D.K. Owens and R.C. Wendt, J. Appl. Polym. Sci. **13,** 1741 (1969).
21. M.P.K. Turunen, T. Laurila, and J.K. Kivilahti, J. Polym. Sci. Part B: Polym. Phys. **40,** 2137 (2002).
22. C. Weast, *CRC Handbook of Chemistry and Physics* (CRC Press, Boca Raton, FL, 1982).
23. J.R. Hollahan and A.T. Bell, *Techniques and Application of Plasma Chemistry* (Wiley, New York, 1974).

24. D.R. d'Agostino, *Plasma Deposition, Treatment, and Etching of Polymers* (Academic Press, San Diego, CA, 1990).
25. D.M. Manos and D.L. Flamm, *Plasma Etching – An introduction* (Academic Press, San Diego, CA, 1989).
26. G. Beamson and D. Briggs, *High Resolution XPS of Organic Polymers* (Wiley, Chichester, 1993).
27. R.J. Good and R.R. Stromberg, *Techniques of Measuring Contact Angles, Surface and Colloid Science* (Plenum Press, New York, 1979).
28. P.S. Swain and R. Lipowsky, Langmuir **14,** 6772 (1998).
29. J. Drelich, J.D. Miller, and R.J. Good, J. Colloid Interface Sci. **179,** 37 (1996).
30. G. Palasantzas and J.M. Hosson, Acta Mater. **49,** 3533 (2001).
31. J. Lawrence, L. Li, and J.T. Spencer, Appl. Surf. Sci. **138–139,** 388 (1999).
32. D.H. Kaelble and K.C. Uy, J. Adhes. **2,** 50 (1970).
33. K.L. Mittal and H.R. Anderson, *Acid-Base Interactions* (VPS, Utrecht, 1991).
34. J.M. Burkstrand, J. Appl. Phys. **52,** 4795 (1981).
35. J.F. Friedrich, W.E.S. Unger, A. Lippitz, I. Koprinarov, G. Kuhn, S. Weidner, and L. Vogel, Surf. Coat. Technol. **116–119,** 772 (1999).
36. L.J. Martin and C.P. Wong, IEEE Trans. Compon. Packaging Technol. **24,** 416 (2001).
37. E. Sacher, J.J. Pireaux, and S.P. Kowalczyk, *Metallization of Polymers,* ACS Symposium Series 440 (ACS, New York, 1990).
38. S. Sapiela, J. Cerny, J.E. Klemberg-Sapiela, and L. Martinu, J. Adhes. **42,** 91 (1993).